

Digital Computer Laboratory
Massachusetts Institute of Technology
Cambridge, Massachusetts

SUBJECT: DEPENDENCE OF COERCIVITY AND STRESS HYSTERESIS ON NUCLEATION OF DOMAINS OF REVERSE MAGNETIZATION

To: David R. Brown

From: John B. Goodenough

Date: May 14, 1953

Abstract: A generalized calculation of the critical field strength for the creation of domains of reverse magnetization at grain boundaries and lamellar precipitates is made. The hypothesis of nucleation of domains of reverse magnetization at lamellar precipitates is able to account for the observed linear variation of coercivity with percent carbon precipitated as lamellar cementite in iron. This is contrasted to a variation to the $2/3$ power with percent carbon precipitated as granular cementite at which closure domains form. The grain boundary contribution to coercivity is calculated and found to depend sensitively on the orientation of the axis of easy magnetization from grain to grain. The variation of coercive force with applied stress is qualitatively explained, and the predicted variations are of the same order of magnitude as is observed. Finally, the concept of nucleation of domains of reverse magnetization at grain boundaries is employed to give a qualitative physical insight into the complicated stress hysteresis phenomena which are observed at different constant field strengths.

I. Introduction

The concept of nucleation of domains of reverse magnetization at grain boundaries which was introduced in E-532¹ is applicable to several phenomena which have not yet been thoroughly understood. The concept can be generalized to include any planar surface with surface pole density w^* (e.g., a lamellar precipitate). A preliminary list of such phenomena

1. J. B. Goodenough and N. Menyuk, Digital Computer Laboratory Engineering Note E-532, M.I.T., March 9, 1953.

includes 1.) the origins of coercivity and its variation with stress and with percent lamellar precipitate, 2.) the stress hysteresis phenomenon at constant field strengths, 3.) the dependence of B-H loop squareness on the magnitude of the spontaneous magnetization, 4.) the dependence of core switching time on grain size or on percent lamellar precipitate, 5.) the qualitative change of shape of the B-H loop with tensile or compressive stress, and 6.) the variation in Bloch wall velocities as measured by a Sixtus-Tonks type experiment from the direct measurements of wall velocities. In this paper, the first two of these phenomena will be discussed. The third and fourth will be discussed subsequently after the completion of a currently projected set of experiments, and the last two were pointed out in E-532.

To generalize the calculation for H_n , the nucleating field strength, to include any planar surface with pole density w^* , the change of crystalline internal energy due to nucleation is

$$\Delta E = (\sigma_o - \sigma_n)A - n[\sigma_w A_w + 2NI_s^2 V - HI_s(\cos \alpha_1 + \cos \alpha_2)V + E_p + E_{np}]$$

as given in Equation (2) of E-532. σ_o and σ_n are the surface energy densities of the planar surface of area A before and after nucleation has taken place. There are n domains of reverse magnetization nucleated each with 180° Bloch wall area A_w , wall surface energy density σ_w , volume V, and demagnetization factor N. α_1 and α_2 are the angles the external field H makes with the spontaneous magnetization vectors of magnitude I_s on either side of the planar surface. E_p and E_{np} are the interaction energies of the magnetic poles associated with the new Bloch walls with, respectively, those on the planar surface and those on neighboring Bloch walls. The nucleation field strength H_n is that field for which the change in free energy, $F = \Delta E - T\Delta S$, between the pre-nucleated and post-nucleated state is zero. To obtain an estimate of the change in entropy of the system with nucleation, it is assumed that the total volume of material V_t is composed of elementary volumes V, where V is the volume of a nucleated domain. Then the total number of such elementary volumes is $N_t = V_t/V$. These may be aligned parallel or antiparallel to their prenucleation direction. The number which align themselves antiparallel at nucleation is $N_d = V_d/V$, where V_d is the volume of material which has reversed its magnetization at nucleation. The entropy change is therefore,

$$\Delta S \cong -k \ln \left(\frac{N_t!}{N_d! (N_t - N_d)!} \right) \cong -N_t k \left\{ p \ln \left(\frac{1}{p} \right) + (1-p) \ln \left(\frac{1}{1-p} \right) \right\}$$

where k is the Boltzman constant and $p = V_1/V_2 \cong 4\pi l / 3b^2 L$. L is a mean grain diameter, $b^2 = A/mR^2$, and $\lambda = R/l$ is the ratio of the minor to major axes of the nucleated domain. The change in free energy is, therefore,

$$\Delta F = \frac{A I_s^2 l}{b^2} \left\{ \gamma_g \lambda - \frac{a \gamma_w}{R} - \gamma \lambda^2 + \gamma_H + \gamma_S \frac{V_E}{R^2 l} \right\} \quad (1)$$

where the dimensionless parameters γ_g , γ_w , γ and γ_H are as given in E-532, and

$$\gamma_S = \frac{3b^2 kT}{4\pi A l I_s^2} \left\{ p \ln \frac{1}{p} + (1-p) \ln \left(\frac{1}{1-p} \right) \right\}$$

The optimum value of n is obtained by setting $\partial(\Delta F)/\partial R = 0$ for a given l . If the resulting relationship between the parameters, viz

$$-\gamma \lambda^2 = \frac{1}{2} \gamma_w \lambda - \frac{1}{2} \frac{a \gamma_w}{R} + \gamma_S \frac{V_E}{R^2 l},$$

is substituted into Equation (1), the nucleation field strength becomes

$$H_m \cong \frac{3b^2 \left\{ \frac{3\pi^2 \sigma_w}{2b^2 \lambda} - \left(\sigma_0 - \frac{\sigma_m}{2} \right) - \frac{2T|\Delta S|}{A} \right\}}{4\pi I_s l (\cos \alpha_1 + \cos \alpha_2)} \quad (2)$$

Typical values for p and N_1/A are $p \sim 0.1$ and $N_1/A \cong L/V \sim 10^{11}$. Therefore at or below room temperature $2T|\Delta S|/A \leq 10^{-3}$ ergs/cm². Since $\sigma_w \sim 0.1$ to 1 erg/cm²,

$$\frac{2T|\Delta S|}{A} / \frac{3\pi^2 \sigma_w}{2b^2 \lambda} \cong 10^{-1} \text{ to } 10^{-2}$$

Although the entropy term will be of increasing importance as the Curie temperature is approached, it is concluded that at and below room temperatures it can be neglected compared to the other terms. Also $\sigma_m \ll \sigma_0$ and is neglected. The nucleation field strength reduces, therefore, to

$$H_m \cong \frac{3b^2 \left\{ \frac{3\pi \sigma_w}{2b^2 \lambda} - \frac{\sigma_0}{\pi} \right\}}{4 I_s l (\cos \alpha_1 + \cos \alpha_2)} \quad (3)$$

This expression is identical with Equation (8) of E-532 if $\sigma_0 = \pi L \omega^{*2}$ is the surface energy density of an infinite, planar grain boundary bounding a grain of length L . Since no grain boundary is an infinite plane, a better approximation for σ_0 can be obtained by calculating

$$\sigma_0 = -\frac{1}{2} \int_0^L H \cdot I_s dz$$

along an axis normal to a grain boundary surface of mean diameter L .

The magnetic field along this axis due to the surface poles of density ω^* is

$$H_z = - \int \frac{\omega^* dS}{z^2 \left(1 + \frac{r^2}{z^2}\right)^{3/2}} = - 2\pi\omega^* z \int_0^{L/2} \frac{r dr}{(z^2 + r^2)^{3/2}} = - 2\pi\omega^* \left\{ 1 - \frac{z}{(z^2 + L^2/4)^{1/2}} \right\}$$

where r is the distance from the foot of the axis to the element of grain boundary area dS . The surface energy density then becomes

$$\sigma_o = \pi\omega^{*2} L G; \quad G = \left\{ 1 + \left(\frac{L'}{2L}\right) - \left[1 + \left(\frac{L'}{2L}\right)^2 \right]^{1/2} \right\}. \quad (4)$$

If θ_1 and θ_2 are the angles made by the normal to the grain boundary with the spontaneous magnetization vectors of magnitude I_s of the adjacent grains, $\omega^* = I_s (\cos \theta_1 - \cos \theta_2)$.

If the planar surface is a lamellar precipitate, then the demagnetization factor is 4π and

$$\sigma_o = - \frac{1}{4} \int_0^{d_l} H \cdot I dz = \pi\omega_\lambda^{*2} d_l. \quad (5)$$

A factor of $1/2$ has entered because the lamellar sheet, of width d_l , has two principal surfaces. If I_p is the magnetization of the precipitate and α_s, α_p are the angles the normal to the lamellar plane makes with the spontaneous magnetizations of the lattice and the precipitate, the lamellar surface pole density is $\omega_\lambda^* = (I_s \cos \alpha_s - I_p \cos \alpha_p)$. The angle α_p will so adjust itself as to minimize the energy associated with ω_λ^* and the anisotropy of the precipitate. The condition that $H_n > 0$ for a lamellar precipitate is, therefore,

$$d_l \omega_\lambda^{*2} < \frac{3\pi\sigma_w}{2b^2\lambda} \sim 0.1401.$$

If $\omega_\lambda^* \sim 7 \times 10^2$, $H_n > 0$ only when $d_l < 5 \times 10^{-6}$ cm. If $\omega_\lambda^* \sim 10^2$, $H_n > 0$ provided $d_l < 10^{-4}$ to 10^{-5} cm. The lamellar precipitate should nucleate domains of reverse magnetization, therefore, in much the same manner as the grain boundary. The H_n for a lamellar precipitate will be negative in metals but may be positive in the ferrites.

II. Coercive Force

The magnetization of a ferromagnetic or ferrimagnetic specimen is changed in an external field by domain creation and/or domain growth. If $H_n < H_c$, the coercivity of the sample is a measure of the resistance to Bloch wall motion within the sample. If the maximum permeability is low, a large proportion of the flux change is due to domain creation and the coercivity is a measure of the smaller resistances to domain wall motion.

The resistance in a material to normal domain wall displacement has several origins. Néel² has discussed the resistances due to inclusions and stress variations within a grain. Whereas Néel considered that the non-magnetic inclusions have magnetic poles on their surface, Williams and Shockley³ have observed closure domains about such inclusions which retard walls which are moving past them with a force proportional to their domain wall surface tension. This mechanism is shown diagrammatically in Figure 1. If the resistance to wall motion is due to the 90° wall surface tension, then

$$2 \underline{H} \cdot \underline{I}_s \Delta V = \sqrt{2} \pi R \sigma_w \Delta x$$

where σ_w , the surface energy density of a 180° domain wall, is taken to be twice that for a 90° wall. If α is the angle between the applied field \underline{H} and the spontaneous magnetization vector \underline{I}_s , if n is the average number of inclusions per cm^2 of 180° domain wall which have closure domains in contact with the moving wall, and if the average radius of the inclusions is $\langle R \rangle$, then

$$H_c = \frac{\pi}{\sqrt{2} \cos \alpha} \left(\frac{\sigma_w}{I_s} \right) \langle R \rangle n.$$

If λ is the mean distance between near-neighbor inclusions, $n \propto \lambda^{-2}$.

If P is the percentage of precipitate in the matrix, it is proportional to the ratio of the volumes of precipitate to total material. Therefore $P \propto \langle R \rangle^3 / \lambda^2$ and $n \langle R \rangle = C_1 P^{2/3} / \langle R \rangle$. For low concentrations the proportionality constant is $C_1 \sim 10^{-1}$. The coercivity is then given by

2. L. Néel, Ann. Univ. Grenoble 22, 299 (1946); Physica 15, (1949); Bull. Soc. Franc. électr. [6] 2, 308 (1949).
3. H. J. Williams and W. Shockley, Phys. Rev. 75, 178 (1949).

$$H_c \sim \frac{1}{4} \left(\frac{\sigma_w}{I_s \langle R \rangle} \right) P^{2/3} \quad (6)$$

Köster's⁴ measurements of the change in H_c with percent carbon in iron which is precipitated as granular cementite are reproduced in Figure 2. The full line is the theoretical curve from Equation (6) for $(\sigma_w / 4I_s \langle R \rangle) = 6$ or $\langle R \rangle \approx 2 \times 10^{-5}$ cm. A $P^{2/3}$ law will prevail only so long as $\langle R \rangle$ does not vary appreciably with percent carbon content. For larger carbon content $\langle R \rangle$ should increase and H_c should fall below a strict $P^{2/3}$ plot.

Köster's measurements of the change in H_c with percent carbon in iron which is precipitated as lamellar cementite is also shown in Figure 2. The variation here is linear with P . Some other mechanism than that of closure domains must be responsible for the forces resisting Bloch wall motion past the lamellar precipitates. If domains of reverse magnetization are nucleated at the lamellar surfaces in the same manner as was postulated for grain boundary surfaces in E-532, then the surface pole energy density which created the Bloch walls will resist their motion. If cylindrical domains of reverse magnetization are nucleated at a planar surface with base radius R in elementary, periodic areas D^2 , the energy associated with the surface magnetic poles is

$$\sigma = \sigma_0 \left| \left(\frac{2\pi R^2}{D^2} - 1 \right) \right| + (\text{Harmonic Terms})$$

At $H = H_c$ the increase in energy associated with the surface magnetic poles must equal the decrease in energy resulting from the increased volume $\Delta V = \Delta [l_m \pi R^2 (\cos^2 \theta_1 + \cos^2 \theta_2)]$ which is aligned in the direction of \underline{H} . The spontaneous magnetization I_s makes an angle θ with the surface normal and l_m is a mean distance between surfaces. If α_1 and α_2 are the angles between \underline{I}_s and \underline{H} , the equilibrium relation $D^2 \Delta \sigma = 2 H_c \cdot I_s \Delta V$ gives for the plane-surface contribution to the coercivity.

$$H_c(\omega^*) = \left(\frac{D^2}{l_m} \right) \frac{d\sigma/dR^2}{\pi I_s (\cos \alpha_1 + \cos \alpha_2) (\cos^2 \theta_1 + \cos^2 \theta_2)} \approx \frac{2\sigma_0}{I_s l_m (\cos \alpha_1 + \cos \alpha_2) (\cos^2 \theta_1 + \cos^2 \theta_2)} \quad (7)$$

The contribution from the harmonic terms is smaller than the contribution from the first term and is neglected.

4. W. Köster, Arch. Eisenhüttenw. 4, 289 (1930).

If the planar surface is a lamellar precipitate, $\sigma_0 = \pi \omega_l^{*2} d_l$ from Equation (5). If the precipitate is cementite, the percentage of carbon in iron is $P \propto (\text{precipitate volume})/(\text{volume of crystal})$. If, therefore, $2 \propto L^2$ is the principal surface area of parallel orientated precipitate in a volume L^3 , then

$$P \propto \frac{d_l \propto L^2}{L^3} = \frac{d_l}{l_m}$$

since the average distance between lamellar areas is $l_m = L/\alpha$. Then, by Equation (7), the contribution to H_c of the lamellar precipitate is

$$H_c(\omega_l^*) = \frac{2\pi C_2 [\langle \omega_l^{*2} \rangle / I_s]}{\langle (\cos \alpha_1 + \cos \alpha_2) \rangle \langle (\cos^2 \theta_1 + \cos^2 \theta_2) \rangle} \cdot P \quad (8)$$

where the proportionality constant is $C_2 \sim 0.04$. The saturation magnetization of cementite is 1000 and of pure iron is 1700.⁵ Therefore $\langle \omega_l^{*2} \rangle / I_s = I_s \langle (\cos \alpha_s - 0.6 \cos \alpha_p)^2 \rangle \sim 100$ Oe. If $2\pi / \langle (\cos \alpha_1 + \cos \alpha_2) \rangle \langle (\cos^2 \theta_1 + \cos^2 \theta_2) \rangle = 3$, then $H_c(\omega_l^*) = 12 P$. This corresponds to the slope of the straight line in Figure 2. Thus the concept of nucleation of domains of reverse magnetization at the lamellar precipitate predicts not only the straight line relationship between H_c and the percent carbon precipitated but also the correct order of magnitude for the slope of the line.

If the planar surface is a grain boundary, $\sigma_0 = \pi \omega^* L G$ from Equation (4). For small angles α_1 , α_2 , θ_1 , and θ_2 the grain boundary contribution to the coercivity becomes [cf. Equation (7)]

$$H_c(\omega^*) \approx \frac{\pi}{2} I_s \langle G(\cos \theta_1 - \cos \theta_2)^2 \rangle \quad (9)$$

If $L' = L$, $G = 1/3$. Since $(\theta_1 - \theta_2) \leq 45^\circ$, a reasonable order of magnitude for the grain boundary contribution to the coercivity in a material whose spontaneous magnetization vectors are not oriented from grain to grain is $H_c(\omega^*) \sim 10^{-3} I_s$. Thus for metals $H_c(\omega^*) \leq 1$ Oe. and for ferrites $H_c(\omega^*) \leq 0.1$ Oe. This contribution can be considerably reduced by the reduction of $\langle G(\cos \theta_1 - \cos \theta_2)^2 \rangle$ through grain orientation, magnetic anneal, or application of tensile stress. If also $L' \ll L$, this factor will be further reduced. This latter condition might be accomplished in large-grained wire specimens in which the grain

5. F. Stäublein and K. Schroeter, Z. anorg. allgem. Chem. 174, 193 (1928).

boundaries constitute cross-sectional areas. Application of a tensile stress of 8Kg/mm^2 to 68 permalloy is shown in Figure 4 of E-532 to cause a decrease in H_c of 0.6 Oe. This is in excellent agreement with the order of magnitude estimate of a $\Delta H_c \lesssim 1$ Oe.

On a saturation loop it is possible for the nucleating field strength H_n to be larger than the field strength required to move domain walls when they exist. If this latter field strength is defined as H_w , then the measured coercivity H_c is either H_n or H_w depending upon which is larger. If $H_c = H_n > H_w$, the B-H loop will have a sharp knee. If $H_c = H_w > H_n$, the B-H loop will not be square. If Equation (7) is substituted into Equation (3), it is at once apparent that a decrease in $(\cos \theta_1 - \cos \theta_2)$ will cause an increase in H_n . From Equation (9), however, a decrease in $(\cos \theta_1 - \cos \theta_2)$ will mean a decrease in $H_c(w^*)$. If, therefore, nucleation occurs at the grain boundaries in a given material in which the directions of spontaneous magnetization can be aligned by tensile stress, H_n should increase and H_w should decrease simultaneously with increasing tensile stress. Sixtus⁶ and Preisach⁷ have made measurements which are capable of distinguishing between H_n and H_w . In their measurements on permalloy, the starting field, H_s , was a measure of H_n whenever $H_c = H_n > H_w$. They also extrapolated a wall velocity vs. driving field curve to zero to define an H_0 . This H_0 represents a resistance to wall motion. One contribution to H_0 , if the hypothesis of grain boundary nucleation is correct for these materials, is $H_c(w^*)$. A plot of H_s and H_0 as a function of applied tensile stress is shown in Figure 3. H_s is seen to rise sharply with increased stress, or decreased $(\cos \theta_1 - \cos \theta_2)$, whereas H_0 decreases. The change in H_0 is nearly 0.3 Oe. This is the predicted order of magnitude of a partially grain oriented specimen.

Thus far in the discussion it has been assumed that the material in question is driven through a saturation cycle. Can the same principles apply if a core is driven around a small B-H loop? If a material with a relatively square B-H loop is driven by an a.c. external field, the sharp knee of the loop will occur at nearly the same field strength as the amplitude of the external field, H_m , is reduced to some value $H_m > H_n$. H_n is taken as that field strength at which the sharp knee occurs. This would

6. K. J. Sixtus, "Probleme der Technischen Magnetisierungskurve" (Springer, Berlin, 1938).

7. F. Preisach, Phys. Z., 33, 913 (1932).

indicate that although some walls are always present in the material when it traverses a small B-H loop, the nucleation and switching mechanism is exactly analogous for the saturation and small loops provided $H_m > H_n$. At small driving fields a smaller fraction of the material is switched.

If a material does not have a relatively square B-H loop, $H_n < H_c(\text{sat.})$ where $H_c(\text{sat.})$ is the coercivity of the saturation loop. If the amplitude of the driving field on such a material is reduced, the ratio R_ϕ of flux change due to nucleation to that due to wall motion during any cycle will increase. If, further, the material has a large magnetostriction coefficient so that the shape of the loop is stress sensitive, the ratio R_ϕ will decrease with an applied tensile or compressive stress which decreases w^* . A decrease in w^* will decrease $H_w = H_c$ and increase H_n . If $H_m > H_c(\text{sat.})$ then the coercivity will reflect the decreased resistance to wall motion and decrease. If, on the other hand, $H_m < H_c(\text{sat.})$, the coercivity will reflect the decrease in R_ϕ with stress. As R_ϕ decreases because more wall motion and less nucleation is taking place, H_c will be a measure of the mean resistance to wall motion of a larger number of walls. It no longer represents the resistance to those few walls which move most easily, and therefore it increases. Hence, a plot of coercivity vs. applied field strength for such a material without and with an applied stress should show an intersection at $H_m \approx H_c(\text{sat.})$. Such measurements have been taken on a Ferroxcube 4B core by P. Baltzer and R. Frackiewicz of this Laboratory and are shown in Figure 4. It should also be noted that the application of 0.32 Kg/mm^2 compressive stress causes a decrease in the saturation coercivity of 0.04 Oe . This is in accord with the order of magnitude estimate of $< 0.1 \text{ Oe}$ for the grain boundary contribution to H_c in the ferrites.

Finally, it should be noted that if sufficient stress is applied so that $H_c = H_n > H_w$, the saturation coercivity will increase with applied stress. Williams⁸ has recently measured the coercivity of a low coercive-force nickel-zinc ferrite body as a function of compressive stress. His curve shows a relatively constant value for $H_c = 0.03 \text{ Oe}$ with $\sigma < 0.65 \text{ Kg/mm}^2$. In this specimen the grain boundary contribution to the coercive force is less than 0.03 Oe . What small variations occur in H_c as a result of decreasing w^* appear to be compensated by increasing internal stresses. At larger

8. H. J. Williams, "Stressed Ferrites having Rectangular Hysteresis Loops," (To be published in E.E.).

compressive stresses such that $H_n = H_c > H_w$ (a sharp knee in the B-H loop appears at this stress value also), the coercivity increases sharply with increased stress. This sharp increase is attributed to the increase in H_n with decrease in $w^* = I_s (\cos \theta_1 - \cos \theta_2)$.

In summary it has been shown that the hypothesis of nucleation at grain boundaries requires that there be a grain boundary contribution to the coercivity. This contribution has been found to vary sensitively with the grain boundary pole density $w^* = I_s (\cos \theta_1 - \cos \theta_2)$. It is especially sensitive to $(\cos \theta_1 - \cos \theta_2)$, or the degree of alignment of the spontaneous magnetization vector on either side of the boundary. This sensitivity and the order of magnitude of the grain boundary contribution are found to be in agreement with experiments on permalloy and on the Ferroxcube 4B ferrite. The variation of H_c , H_s , and H_o with stress in permalloy and the nickel-zinc ferrite are in good qualitative agreement with the hypothesis that $H_c = H_n$ or H_w (whichever is the larger), and the predicted variations of H_n and $H_c(w^*)$. Finally the hypothesis of nucleation of domains of reverse magnetization at lamellar precipitates has predicted a linear variation of H_c in iron with percent carbon precipitating as lamellar cementite. This is in agreement with the measurements of Köster⁴ and in contrast to the variation with percent carbon to the 2/3 power for granular cementite at which closure domains prefer to form.

III. Stress Hysteresis

Since the work of Ewing⁹ before the turn of the century stress hysteresis in ferromagnetic materials at constant field strength has been observed, but no satisfactory explanation of this phenomenon has heretofore been offered. The hypothesis of nucleation at grain boundaries, however, provides a simple, qualitative explanation for this apparently complex phenomenon. Besides rotation of the spontaneous magnetization vectors in the applied field, there are two principal mechanisms which are responsible for flux change in a magnetic material, viz. domain creation and Bloch wall movement. Each of these may be either reversible or irreversible. If a

9. J. H. Ewing, "The Electrician" (London, 3d Ed., 1900).

tensile or compressive stress σ is applied, the resulting magnetostrictive forces favor a single direction of easy magnetization throughout the material which is determined by the direction of σ . In a polycrystalline material with a positive magnetostriction constant, such as permalloy, the spontaneous magnetization vectors of the individual grains are rotated toward the direction of applied tensile stress. The surface pole density at the grain boundary, $w^* = I_s (\cos \theta_1 - \cos \theta_2)$, decreases as the alignment of the spontaneous magnetization vectors improves. Since the Bloch wall surface energy density does not vary as rapidly as w^* , H_n will increase by Equations (3) and (4). The range of variation in $(\cos \theta_1 - \cos \theta_2)$ over the various grain boundaries will be decreased. The number of nucleated domains as a function of H will, therefore, be shifted to higher field strengths and be concentrated over a smaller range of H . A decrease in w^* will also mean a decrease in $H_c(w^*)$ by Equation (9). Bloch walls which are present in a material will move under a smaller driving field H . In summary, then, the hypothesis of nucleation at grain boundaries predicts that the change of an applied stress which alters w^* in the presence of a given external field strength H will have two important effects. 1.) If the field strength required for motion of a wall is decreased by a decrease in w^* below the given field strength H , the domain will grow or contract according to its orientation with respect to H . 2.) The number of nucleated domains for a given H will vary with the value of w^* . If a decrease in w^* makes $H_n < H$, the surface tensions in the Bloch walls will exceed the net force to maintain domains of reverse magnetization which are nucleated at grain boundaries. There results a net force to shrink these domains to zero volume.

Figure 5 shows a B-H loop of 68 Permalloy¹⁰ which was taken with a stress $\sigma = 4\text{Kg/mm}^2$ continually maintained (broken line) and a loop (solid line) with the same stress released and then reapplied at various constant values of H marked (i) - (ix). Figure 6 shows a similar loop¹⁰ taken with no stress applied except at certain values of H at which it is applied and subsequently released.* The resulting changes in the magnitude of the induction can now be qualitatively understood.

10. R. M. Bozorth, "Ferromagnetism" (D. Van Nostrand Co. Inc., 1951), Chapter 13.

* This data was called to my attention by P. K. Baltzer.

When the stress was released at (i) of Figure 5, the direction of easy magnetization was no longer aligned by the stress and the spontaneous magnetization vectors of the individual grains rotated to a set of axes which were determined by the crystallographic orientation of the grains. The contribution to the flux change due to this rotation is reversible and small compared to the observed flux change of nearly a factor of six. The change of flux due to such rotations will not be mentioned in the subsequent discussion. It will be understood that this contribution is always present. The significant feature for this discussion is that w^* increased when the stress was removed. Apparently w^* increased sufficiently to make $H_n < H(i)$. There resulted a nucleation of many domains of reverse magnetization at the grain boundaries with a resultant large decrease in the induction through the sample. When σ was reapplied, w^* decreased again and $H_n > H(i)$. Since also $H(i)$ was opposed to the formation of reverse domains, the domains which had been created when σ was released disappeared when σ was reapplied. There were a few domains which were irreversibly created, however, so that the induction through the sample was not completely regained by the reapplication of σ .

At (ii) and (iii) the process was the same as at (i) except that more domains of reverse magnetization were irreversibly created. This is quite consistent with the fact that $H(i)$ was opposed to the existence of reverse domains, $H(ii) = 0$, and $H(iii)$ favored their existence. The field $H(iii)$ favored the formation of larger domains and opposed the Bloch wall surface tension forces which were acting to destroy the new domains when the stress was reapplied. It is interesting to note that the history of the specimen affected its coercivity. After release and reapplication of stress at (iii), there were many irreversibly formed reverse domains present. Their existence altered the distribution of w^* over the grain boundaries so as to reduce the number of new domains nucleated at increased values of H . More Bloch wall motion was necessary to reduce the induction to zero, and the coercivity was consequently slightly increased.

At (iv) there was, initially, a large percentage of the specimen's volume within domains antiparallel as well as parallel to $H(iv)$. When σ was released, the increase in w^* caused the nucleation of domains with orientations parallel or antiparallel to $H(iv)$ depending upon the orientation of the larger domain in which they were formed. Although those which were

oriented parallel to $H(iv)$ should have been larger, on the average, than those oriented antiparallel to $H(iv)$, fewer of them were formed. There resulted a decrease in the induction as shown. When σ was reapplied, however, the domains which were created antiparallel to $H(iv)$ disappeared with decreasing w^* . Since $H(iv) > H_c (\sigma = 4\text{Kg/mm}^2)$, those which were created parallel to $H(iv)$ remained and even grew. The marked increase in $|B|$ resulted.

The mechanisms at (v) and (ix) were the same as at (iv) except that the proportion of created domains which were oriented parallel to H was greatly reduced. The mechanisms at (vi) and (vii) were the same as those at (i), (ii), and (iii).

When σ was released and w^* increased at (viii), the majority of new domains were oriented parallel to $H(viii)$. A sharp decrease in $|B|$ resulted. Since $H(viii) \approx H_c (\sigma = 4\text{Kg/mm}^2)$, when σ was reapplied, the favorably oriented new domains grew while the unfavorably oriented ones disappeared. Consequently $|B|$ continued to decrease until the induction changed sign and increased in the apposite direction.

The nine steps in the hysteresis loop of Figure 6 can be understood in an analogous manner. Initially the domain structure was complex with nearly as many domains oriented antiparallel as parallel to H . When σ was applied at (i), the resulting decrease in w^* favored a simpler domain structure. Consequently most of those domains which were oriented antiparallel to H disappeared and the induction markedly increased. When w^* was subsequently increased by the release of σ , domains of reverse magnetization were formed at the grain boundaries since $H_n < H(i)$. Because of the very different history of formation of the original reverse domains from that of those created at the grain boundaries by the release of the stress, the induction did not return to its original value. The original volume included within reverse domains was more extensive because the original magnetizing field was much smaller than $H_c (\sigma = 0)$ so that little wall movement could take place to alter the domain pattern from that of the completely demagnetized state.

Because of the application and release of stress at (i), at (ii) the specimen consisted primarily of large domains, oriented more or less parallel to the original field, in which existed many small domains of oppositely directed magnetization. When σ was reapplied at (ii), therefore,

the small domains, most of which were reversibly formed, disappeared as w^* decreased. Since $H(ii) = 0$, there was no external field to aid in shrinking the reverse domains. The induction at (ii) with $\sigma = 4\text{Kg/mm}^2$ could, therefore, have been no larger than the corresponding value at (i). Because some of the reverse domains were irreversibly created, the induction at (ii) with $\sigma = 4\text{Kg/mm}^2$ was slightly less than that at (i). Since only the reversibly created domains disappeared when σ was applied, the release of σ caused the recreation of the original reverse domains and the induction returned to its original value.

$H(iii)$ was parallel to the reverse domains which were nucleated at (i) and (ii) when the stress was released. When σ was applied at (iii), therefore, $H(iii)$ opposed the collapse of many of the nucleated domains. Since $H(iii)$ was nearly equal to the field strength at the first knee of the $\sigma = 4\text{Kg/mm}^2$ curve (a field strength at which nucleation apparently took place), it was of sufficient magnitude to oppose the collapse of those domains which would have been created at the first knee. The increase in induction with applied stress was, therefore, considerably smaller at (iii) than it was at (i) and (ii). Because $H_c(w^*)$ was reduced, $H(iii)$ was not only strong enough to oppose the collapse of some of the reverse domains, but also capable of causing them to grow somewhat. When σ was removed, therefore, the induction decreased below its original value upon renucleation of the reverse domains.

$H(iv) > H_c(\sigma = 4\text{Kg/mm}^2)$. When the stress was applied at (iv), the coercivity was reduced to where the nucleated domains could grow to reverse the induction through the sample. When σ was released, domains were nucleated antiparallel to $H(iv)$ in the then large domains oriented parallel to $H(iv)$. Consequently $|B|$ decreased, but the direction of the induction remained reversed.

$H(v)$ was sufficiently large that the reduction in w^* and in $H_c(w^*)$ with applied stress caused the domains antiparallel to $H(v)$ to disappear and those parallel to $H(v)$ to grow until they occupied most of the specimen volume. Although domains antiparallel to $H(v)$ were created when w^* increased at the release of σ , the induction was increased by the application and removal of stress.

As the magnitude of the applied field was decreased from $H(v)$ to $H(vi)$, more and more domains were nucleated antiparallel to H . When the

stress was applied at $H(v_i)$, there was not sufficient energy released to cause all of these nucleated domains to disappear. The existing domain walls which were at an equilibrium position with the driving force $H(v)$ at $\sigma = 4 \text{ kg/mm}^2$ remained in this position when σ was released. They did not move when H was reduced with $\sigma = 0$ because of the large resistance to wall motion from the grain boundary poles. When σ was applied at $H(v_i)$, however, the resistance to wall motion was reduced and these walls could relax to a position of equilibrium with the smaller driving force $H(v_i)$. As a result the induction with σ applied was smaller at $H(v_i)$ than at $H(v)$ and was reduced slightly below its pre-stressed value at (v) when σ was released.

The mechanisms responsible for the induction changes at (vii), (viii), and (ix) are essentially those of (iii), (iv), and (v). Thus the hypothesis of nucleation at grain boundaries with its resulting requirement that the nucleation field strength increase and the resistance to wall motion decrease with decreasing w^* has permitted some physical insight into the mechanisms responsible for the complicated stress hysteresis patterns at constant field strength which have been observed in permalloy. Figures 7 and 8 show similar curves which were made on a Ferroxcube 4B sample.¹¹ Here the magnetostriction constant is negative and compressive stresses were used to reduce w^* . The argument for these curves is completely analogous to that for the 68 permalloy curves. The degree of change is, in this case, less spectacular both because the stresses used were not so large and because I_s is much smaller for the ferrite so that the magnitude of change in w^* with change in $(\cos \theta_1 - \cos \theta_2)$ is reduced. The curves do support, however, the concept of nucleation at grain boundaries in the nickel ferrites as well as the permalloys.

In Figure 9 are shown¹⁰ the effects on the initial magnetization curve for 68 permalloy of applying the tensile stress σ and the magnetizing field H in different orders. Curve (a) is the normal initial magnetization curve. Since w^* is large, $H_c(w^*)$ is large. For $H < 0.1 \text{ Oe.}$, therefore, there is little Bloch wall motion, and the permeability remains low. Curve (b) is the initial magnetization curve when the specimen is subject to a tensile stress $\sigma = 4 \text{ kg/mm}^2$. Since the tensile stress reduces $(\cos \theta_1 - \cos \theta_2)$,

11. P. K. Baltzer and R. Frackiewicz, Digital Computer Laboratory, MIT.

$H_c(w^*)$ is reduced to where the total coercivity is $H_c = 0.042$ Oe. Therefore at $H = 0.1$ Oe., most of the domain wall motion has taken place. Since the spontaneous magnetization vectors are largely aligned by the stress and the wall motion is nearly completed, the induction increases to nearly its saturation value at $H = 0.1$ Oe. only.

Curve (d) traces the initial magnetization when the field H is applied before the stress. If σ is applied to reduce w^* , the domain wall surface tension will exceed the field strength necessary to maintain the small domains nucleated at the grain boundaries. These excess surface tensions will cause the domain wall area to decrease. If a field H has been applied prior to σ , those domains which are aligned antiparallel to H will be the most likely to disappear. Even at field strengths $H < H_c$ ($\sigma = 4\text{Kg/mm}^2$), the sum of the excess surface tensions and the applied field will be sufficient to collapse nearly all of the domains antiparallel to H . The initial permeability is therefore extremely large and the initial magnetization curve rises sharply to nearly the saturation value. The excess domain wall surface tensions do not exist if the material is demagnetized under a tensile load and then magnetized without removing the stress, as in curve (b).

If the stress is applied and then released after the field H has been applied, the initial magnetization curve traces out the curve (c). When the stress is released, the magnetization drops from curve (d) to curve (c) because of the nucleation of domains of reverse magnetization within the large domains oriented parallel to H . The initial permeability is high because the domains which are nucleated antiparallel to H when σ is released occupy considerably less than half the volume whereas the original domains oriented antiparallel to H occupied, from curve (a), nearly half the total volume of the specimen.

A completely analogous set of initial magnetization curves for the Ferroxcube 4B body under a compressive stress of 0.32 Kg/mm^2 are shown¹¹ in Figure 10. In Figure 11 is shown the effect on the B - H loop of 68 permalloy of applying and removing a tensile stress $\sigma = 4\text{Kg/mm}^2$ twice at various field strengths. The normal loop (no tension) has a remanence $B_R < B_s/5$. If rotation of the spontaneous magnetization vectors of the individual grains from the direction of the applied field to an axis of easy magnetization were alone responsible for the change in induction ($B_s - B_R$), the remanence should be some $B_R \geq B_s/2$. Nucleation of domains of

reverse magnetization must be contributing to the decrease in induction. This conclusion is quite consistent with the argument in connection with Figures 5 and 6 where it was assumed that $H_n < 0$ if $\sigma = 0$. If the stress $\sigma = 4\text{Kg/mm}^2$ is applied at any H , the coercivity of the sample is, by Figure 9, reduced to 0.042 Oe. Also, the consequent reduction in W^* which increases the nucleation field strength (c.f. Figure 5 and 6) to $H_n \approx 0.02$ Oe. results in a minimization of the number of Bloch walls present in the specimen. If a field $H \geq 0.042$ Oe is present, the domains oriented antiparallel to H will shrink or disappear, those oriented parallel to H will grow. The degree to which the walls completely disappear depends, of course, on the magnitude of H . When the stress is removed, domains antiparallel to H will be created in the large domains parallel to H , and the induction will be reduced. The effect on the B-H loop of 68 permalloy of application and removal of $\sigma = 4\text{Kg/mm}^2$, therefore, is the reduction in the coercivity from an $H_c > 0.4$ Oe. to an $H_c \approx 0.042$ Oe. The remanence is affected comparatively little since the domains which shrink or disappear when σ is applied in a field $H = 0$ reappear when σ is released. After the stress σ is applied, however, some domain walls are still present in the specimen. If the resistance to wall motion is reduced by the application of stress, these relax to a position of equilibrium with $H = 0$ instead of with $H = 5$ Oe. When the stress is subsequently released, these walls remain in their new position. The value of B_R is, consequently, slightly reduced by the application and removal of σ .

If H is applied first and maintained constant during a successive application and removal of tensile or compressive stress on a specimen, the successive values of induction in the stressed material decay to some constant value. This effect is more pronounced in the stress sensitive materials. Figure 12 shows¹⁰ the change of induction in a 68 permalloy sample in a field of 0.14 Oe. caused by repeated application and removal of a tension of 4Kg/mm^2 . Since $H_n < -0.14$ Oe., many domains of reverse magnetization are nucleated when the tension is released. Although the field $H = 0.14$ Oe. tries to inhibit the size of these domains, nevertheless a certain fraction of these domains can form irreversibly by colliding with one another. When the stress is reapplied, therefore, not all of the domains which were created disappear. The distribution of grain boundary magnetic pole density is now different when the stress is again released. The domains of reverse magnetization are not nucleated in the same positions and more of the created

domains can form irreversibly. With each successive application and release of stress, however, the probability of forming new irreversibly nucleated domains of reverse magnetization is diminished. The change in induction rapidly approaches a "cyclic state" which represents the change due to reversible nucleation and annihilation of domains of reverse magnetization with change in w^* by change in stress.

Figure 13 shows¹¹ the change in induction in a Ferroxcube 4B sample in a field of 0.65 Oe. caused by successive application and removal of a compressive stress of 0.32 Kg/mm². The core was first magnetized in a field 4.3 Oe. in the opposite direction so that, cf. Figure 7, in the field 0.65 Oe. the induction in the sample has been brought over the sharp knee of the B-H loop but, since $H_c \approx 0.76$ Oe., is initially still antiparallel to the applied field. When the stress was first released, therefore, the resulting nucleated domains were predominately oriented parallel to H. The induction decreased markedly. When the stress was reapplied, most of the just created domains antiparallel to H disappeared along with some of those parallel to H. The field $H = 0.65$ Oe., however, was strong enough to capture some of the newly nucleated domains. In fact, with the decrease in $H_c(w^*)$ with stress, these newly created domains which were captured by H also grew. There resulted a further decrease in induction. When the process was repeated, the proportion of initial material antiparallel to H was considerably smaller so that the net effect was reduced. Successive application and removal of stress contained a greater and greater proportion of reversible change. Before the "cyclic state" was reached, however, the direction of induction in the sample had been reversed to become parallel to the applied field.

Figure 14(a) shows a diagrammatic sketch of the disturbed pulses observed in the output from a memory core. A corresponding B-H loop is shown in Figure 14(b). The explanation for the change in successive disturb signals is completely analogous to the decay in induction change with repeated applications of stress. Here, however, nucleation is not accomplished by a change in w^* , but by a change in H. At first both reversible and irreversible nucleation takes place when the disturb signal is on. The proportion of irreversible nucleation, however, decays quickly to zero.

In summary, the concept of nucleation of domains of reverse magnetization at grain boundaries which predicts an increasing nucleation field strength and a decreasing resistance to wall motion as the grain boundary magnetic pole density decreases has suggested a qualitative physical insight to the complicated induction changes which occur in ferromagnetic materials when they are subjected to changes in tensile or compressive stress.

Signed John B. Goodenough
John B. Goodenough

Approved JAB

JBG/jk

cc: Group 63

Drawings attached:

Figures 1,2 A-55088
Figure 3 A-55089
Figure 4 A-55090
Figure 5 A-54747
Figure 6 A-55083
Figure 7 A-55080
Figure 8 A-55081
Figure 9 A-55082
Figure 10 A-55162
Figure 11 A-55163
Figure 12 A-55101
Figure 13 A-55102
Figure 14 A-55164

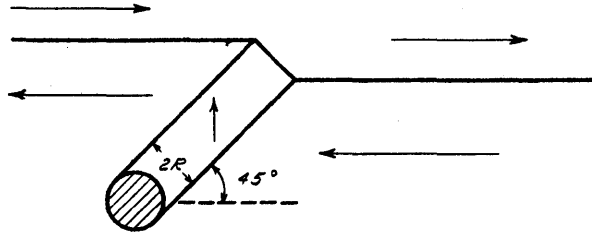


FIG. 1

DOMAIN STRUCTURE AROUND AN INCLUSION
BEFORE THE CONNECTION BETWEEN CLOSURE DOMAIN
AND MOVING 180° WALL IS BROKEN

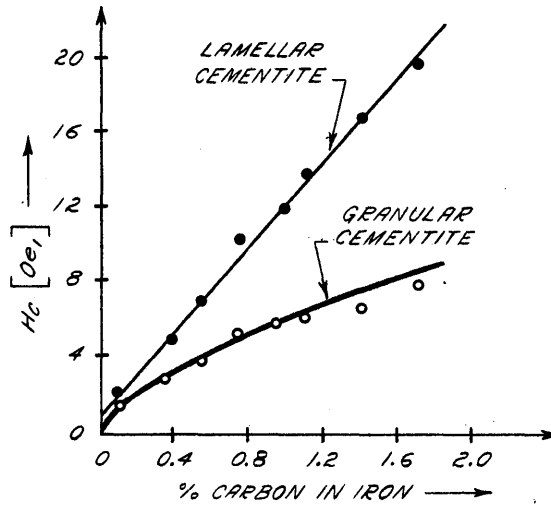


FIG. 2

DEPENDENCE OF H_c ON THE AMOUNT OF CARBON IN IRON
IN THE FORM OF GRANULAR AND LAMELLAR CEMENTITE

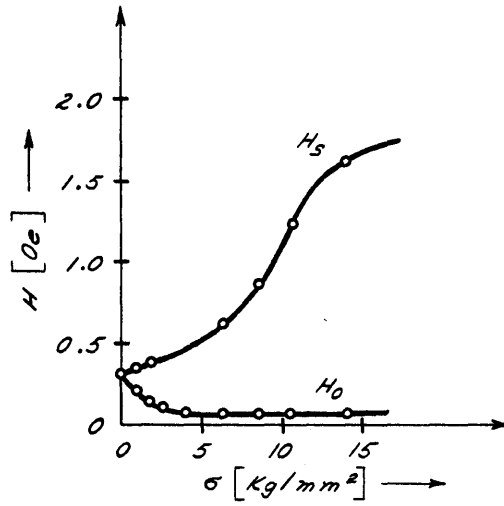


FIG. 3

H_0 AND H_s VS. APPLIED TENSILE STRESS
 FOR A 78.5 PERMALLOY ROD ANNEALED 5 MIN.
 AT 800°C IN VACUUM

A-55089

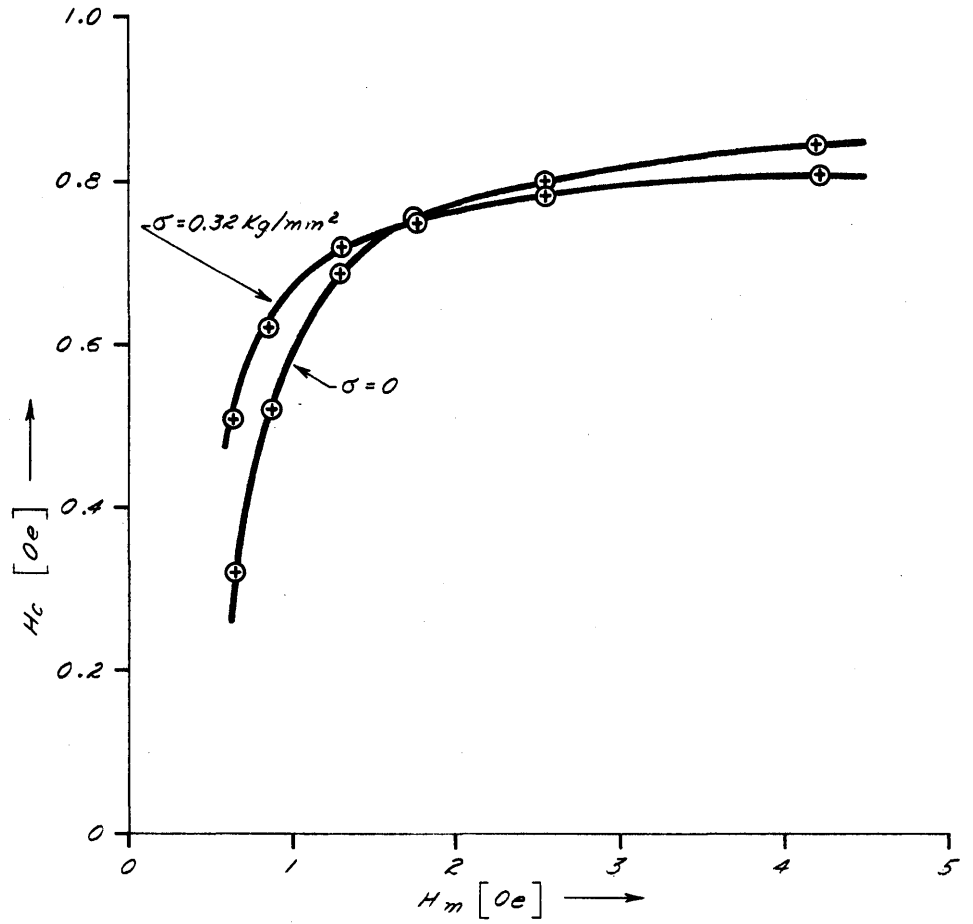
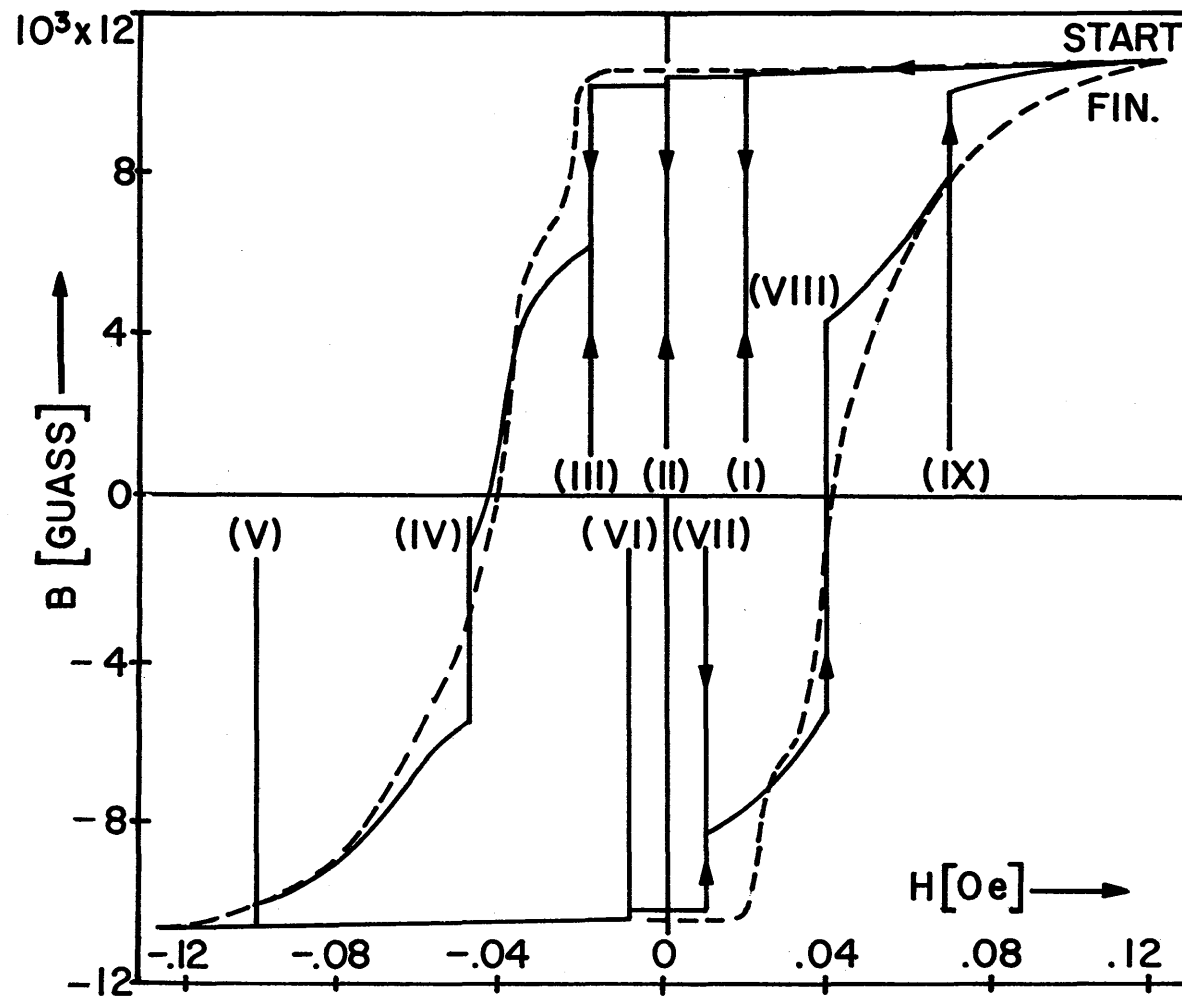


FIG. 4

H_c VS. MAXIMUM APPLIED FIELD STRENGTH
FOR A FERROXCUBE 4-B CORE WITHOUT
AND WITH AN APPLIED COMPRESSIVE STRESS

A-54747
F-1912
S-564



HYSTERESIS LOOP OF 68 PERMALLOY
UNDER 4 kg/mm^2 TENSION FIG. 5

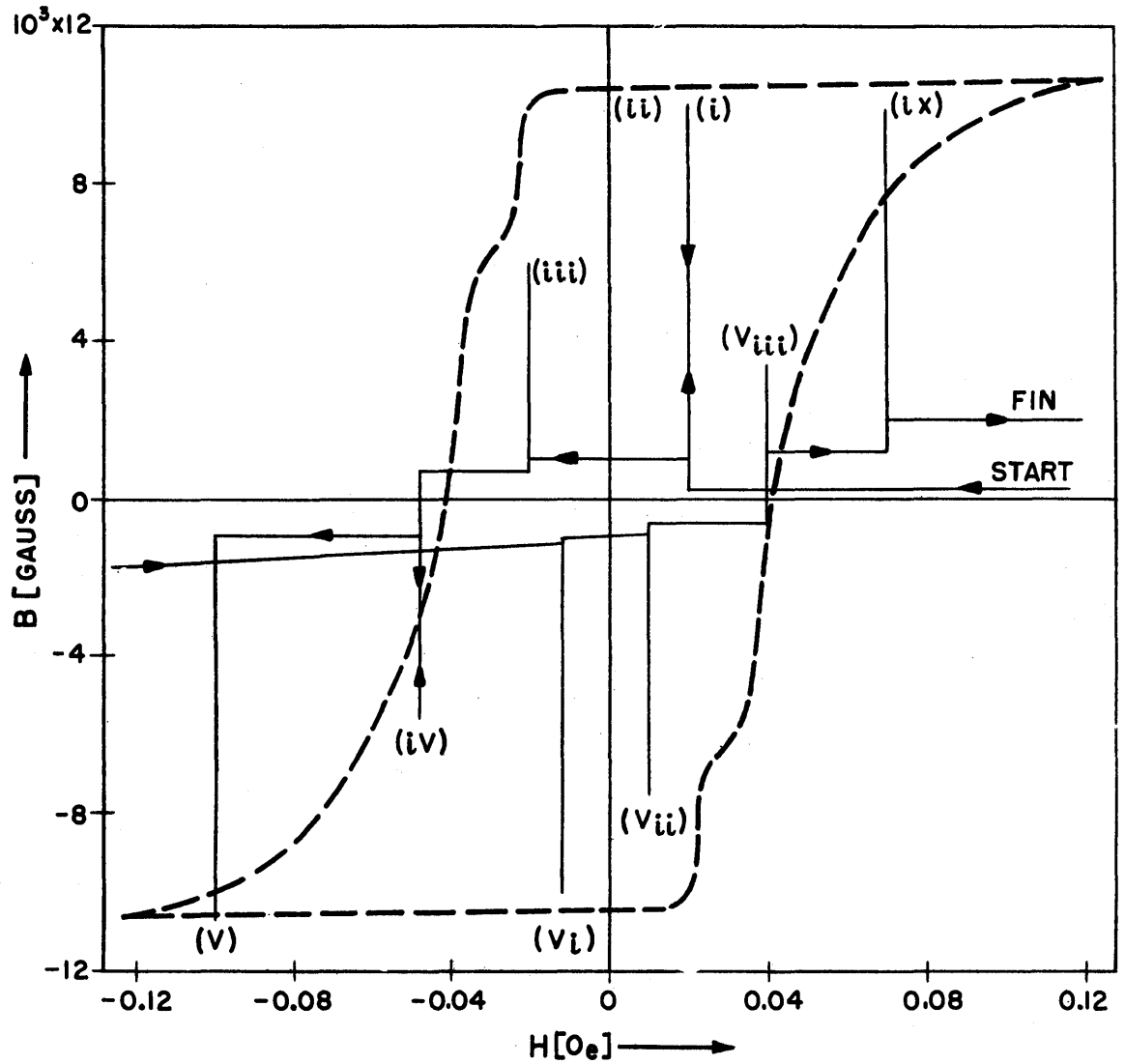


FIG. 6
 HYSTERESIS LOOP OF 68 PERMALLOY.
 TENSION ZERO EXCEPT WHEN 4 Kg/mm² APPLIED
 AND REMOVED AT CERTAIN FIELD STRENGTHS.

A-55083

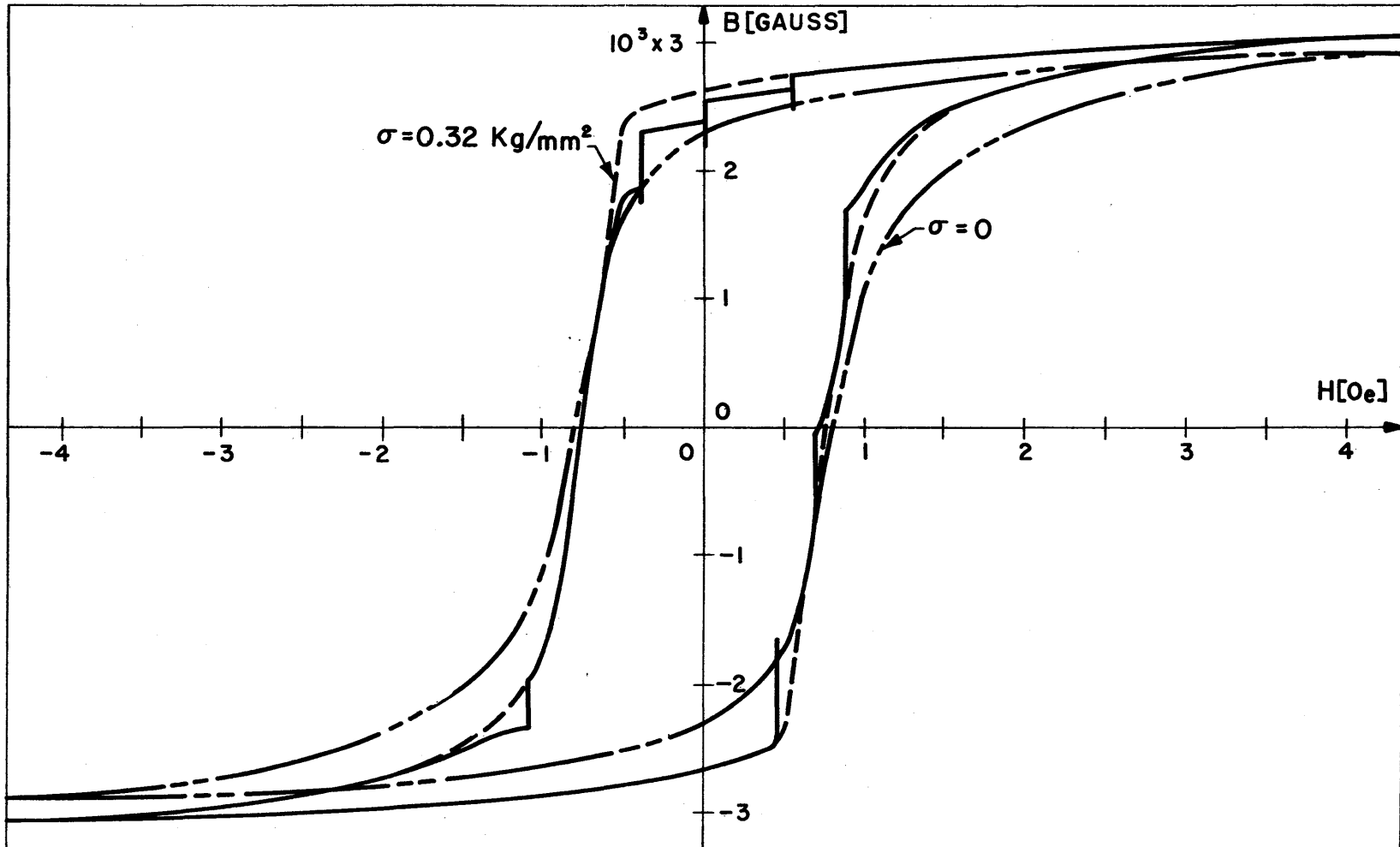


FIG. 7
 HYSTERESIS LOOP FOR FERROCUBE 4-B. COMPRESSION 0.32 Kg/mm^2 EXCEPT
 WHEN REMOVED AND REAPPLIED AT CERTAIN FIELD STRENGTHS.

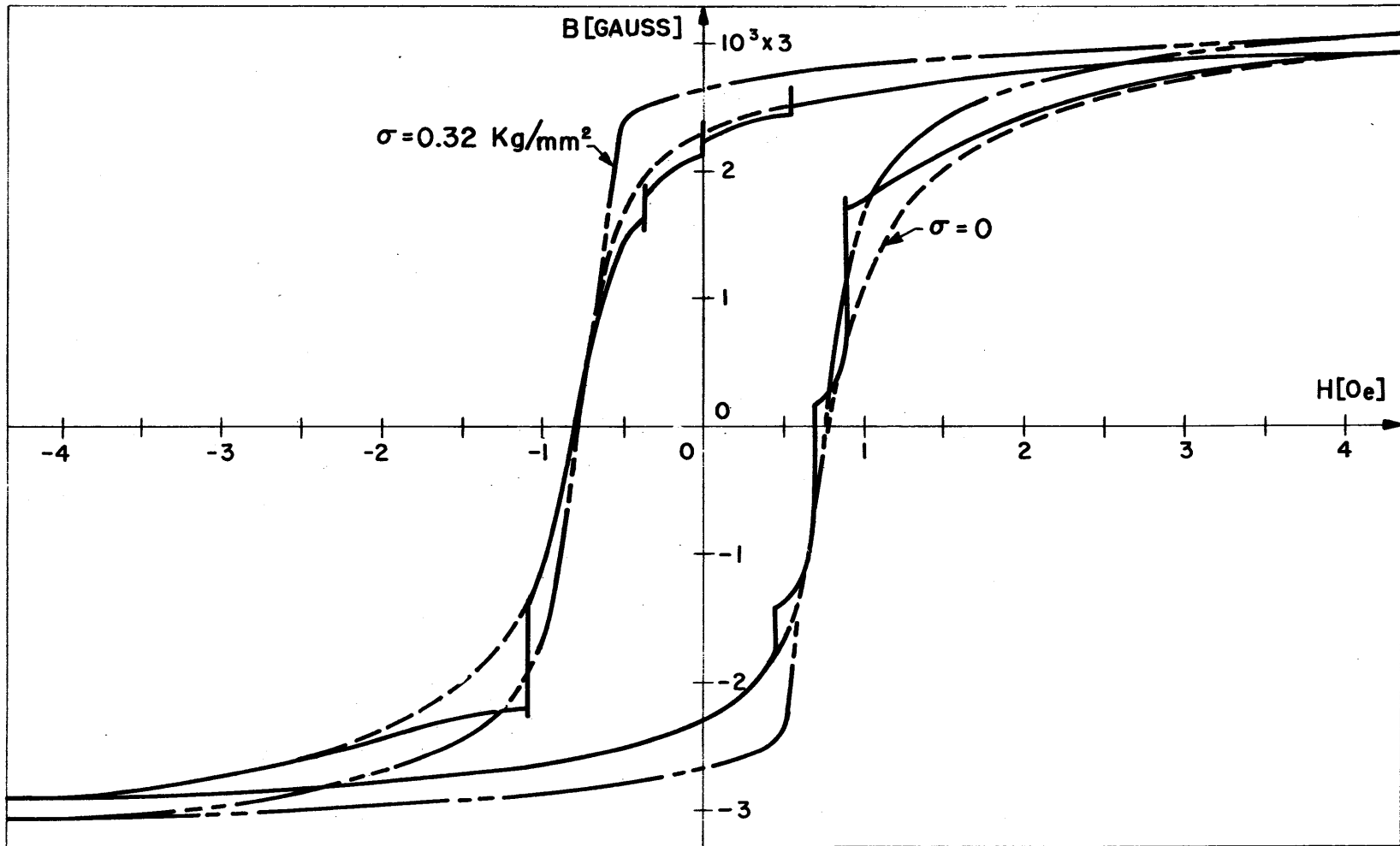
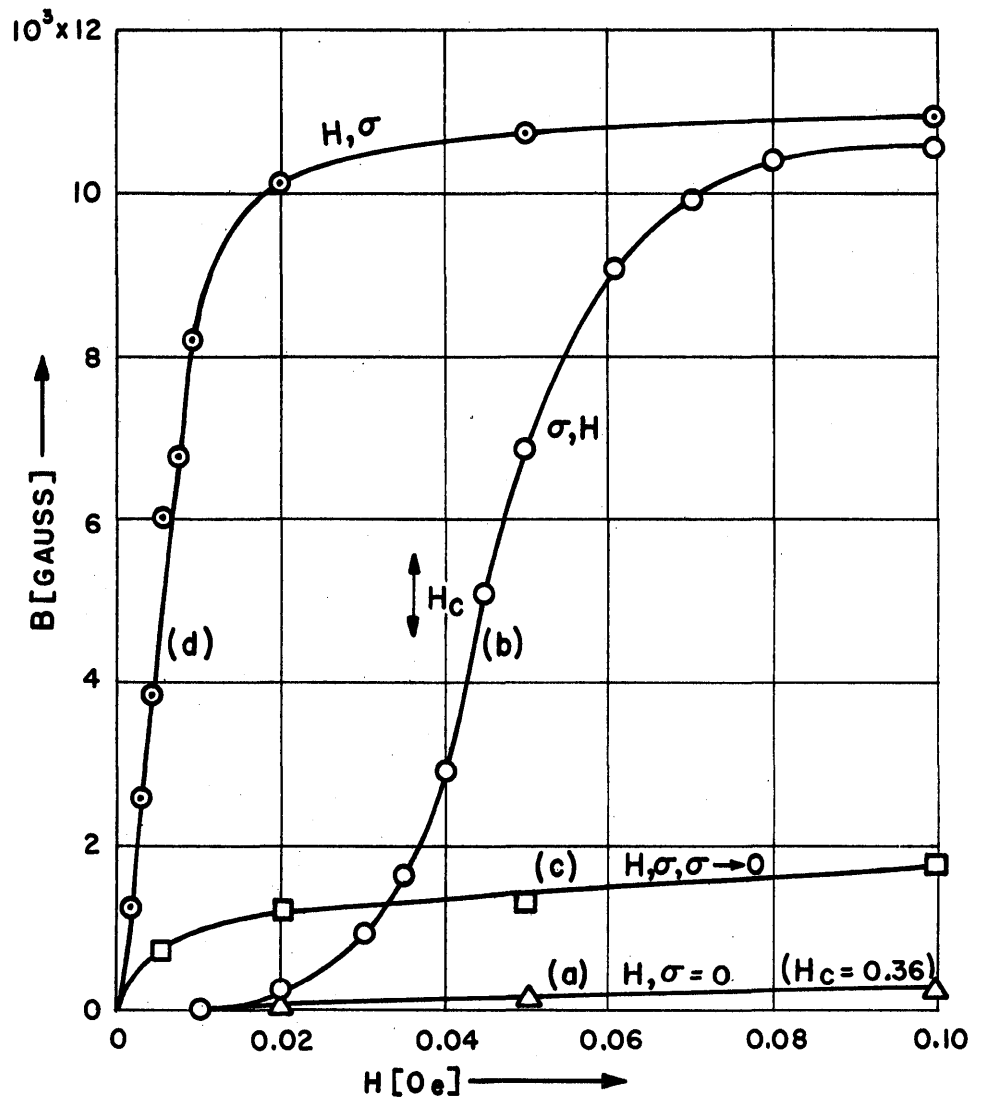


FIG. 8

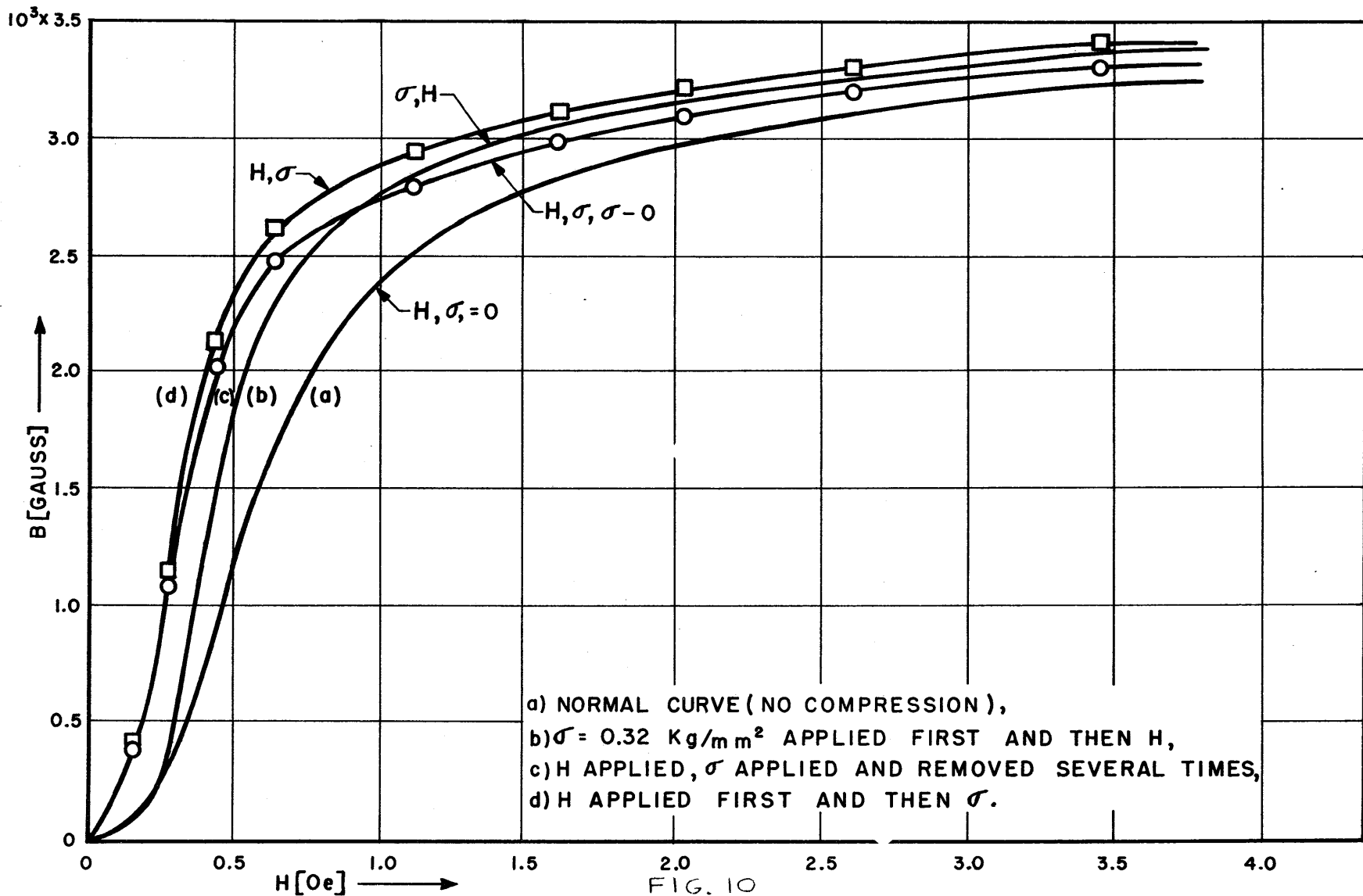
HYSTERESIS LOOP FOR FERROXCUBE 4-B. COMPRESSION ZERO EXCEPT WHEN 0.32 Kg/mm² APPLIED AND REMOVED AT CERTAIN FIELD STRENGTHS.



- a) NORMAL CURVE NO TENSION.
 b) σ (4 Kg/mm²) APPLIED FIRST AND THEN H.
 c) H APPLIED, σ APPLIED AND REMOVED SEVERAL TIMES.
 d) H APPLIED FIRST AND THEN σ .

FIG. 9

VARIOUS KINDS OF MAGNETIZATION CURVES
 OF 68 PERMALLOY



a) NORMAL CURVE (NO COMPRESSION),
 b) $\sigma = 0.32 \text{ Kg/mm}^2$ APPLIED FIRST AND THEN H ,
 c) H APPLIED, σ APPLIED AND REMOVED SEVERAL TIMES,
 d) H APPLIED FIRST AND THEN σ .

VARIOUS INITIAL MAGNETIZATION CURVES FOR FERROXCUBE 4-B

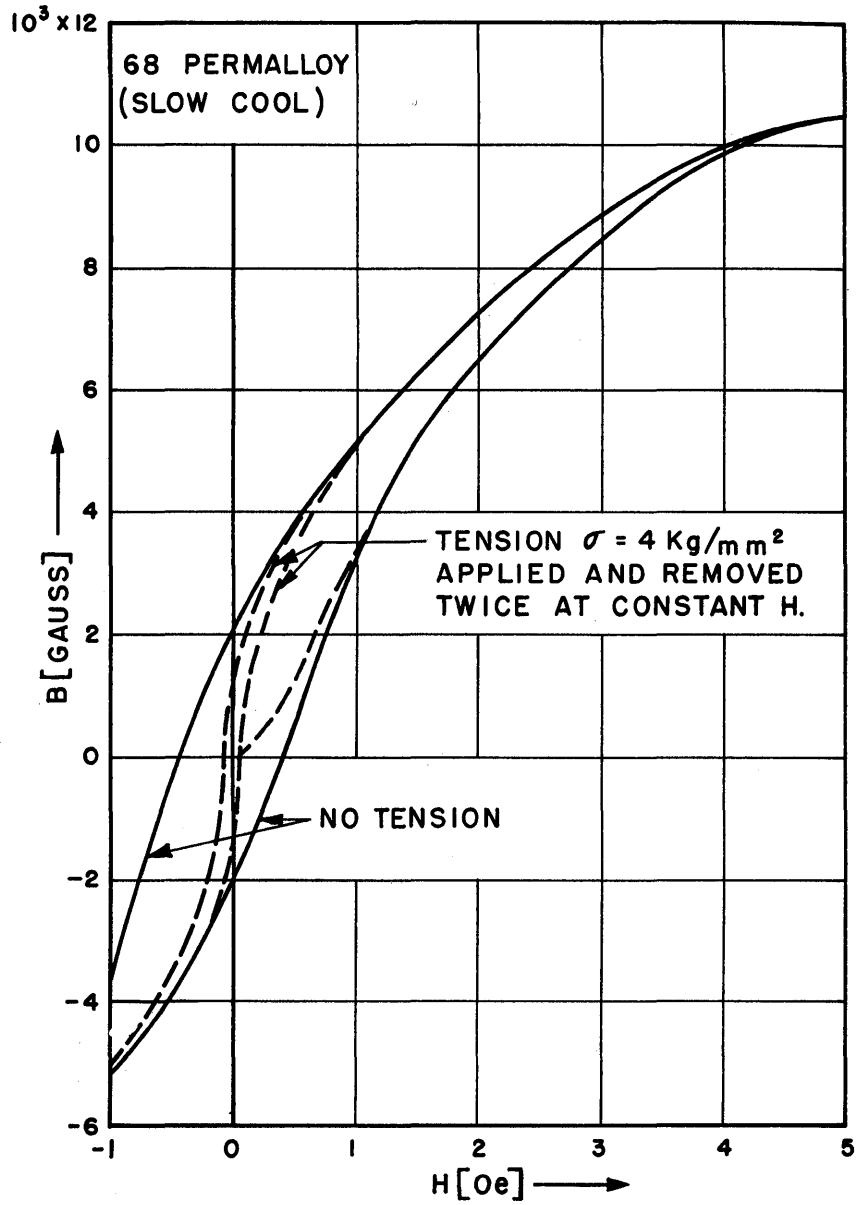


FIG. 11
EFFECT OF APPLYING AND REMOVING A TENSION
 $\sigma = 4 \text{ Kg/mm}^2$ TWICE AT VARIOUS CONSTANT
FIELD STRENGTHS ON THE HYSTERESIS
LOOP OF 68 PERMALLOY

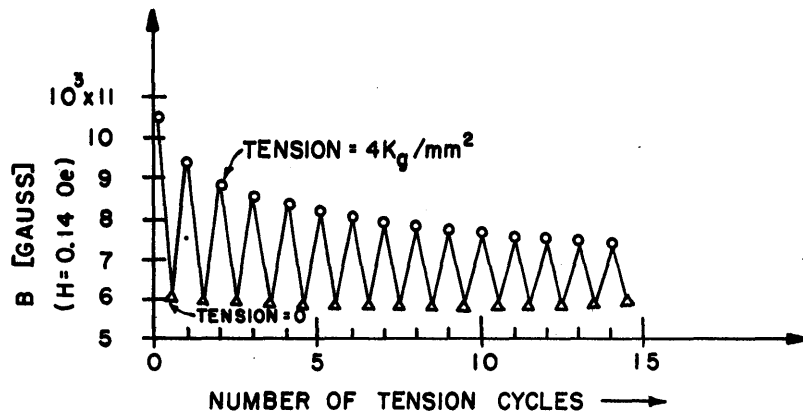
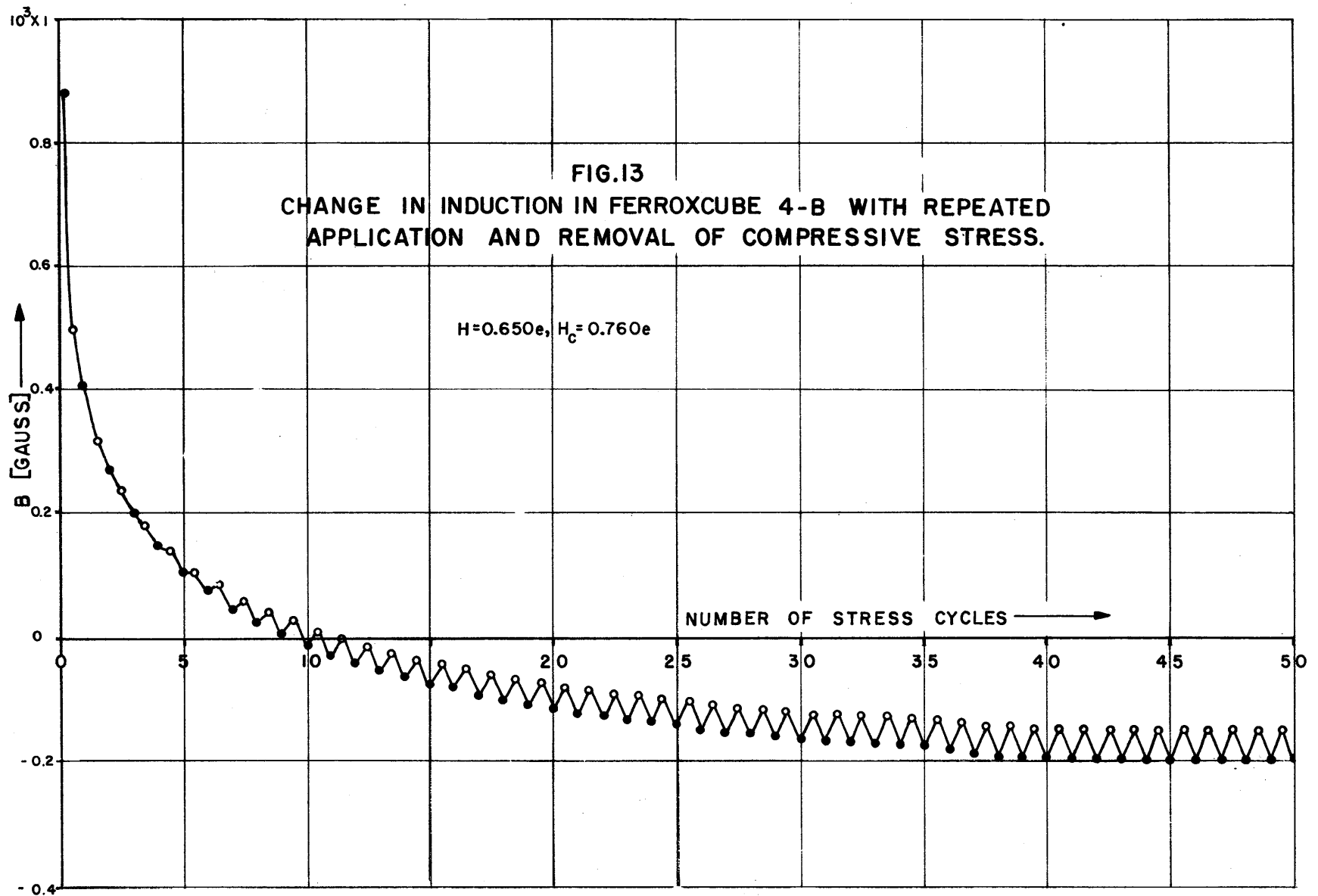


FIG. 12
CHANGE AT INDUCTION CAUSED BY REPEATED
APPLICATION AND REMOVAL OF A TENSION
OF 4Kg/mm² IN 68 PERMALLOY.



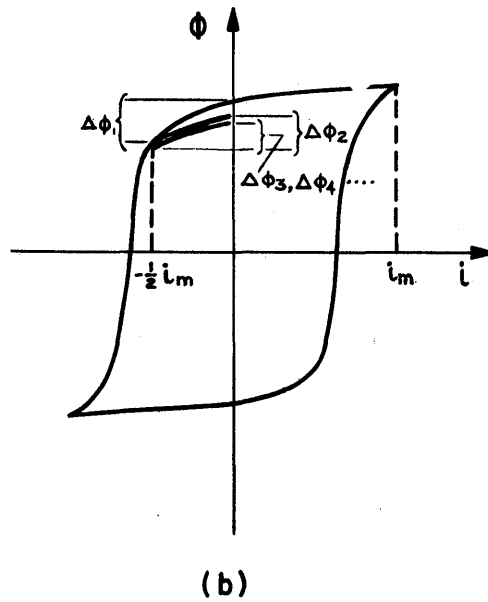
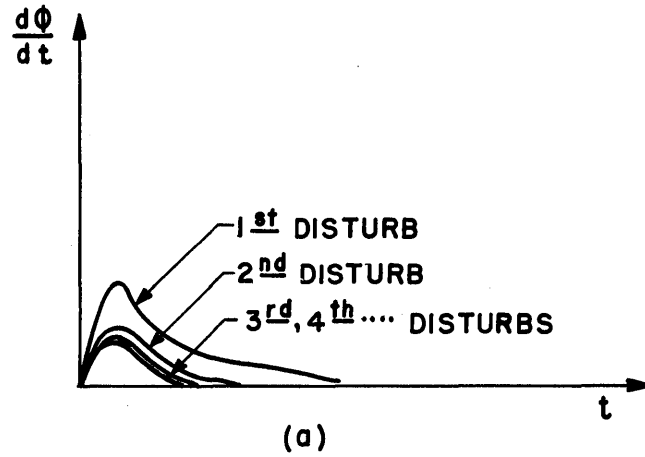


FIG. 14

DIAGRAMATIC VOLTAGE OUTPUT FOR A TYPICAL SQUARE-LOOPEd MATERIAL DRIVEN BY A SERIES OF HALF AMPLITUDE, "DISTURB", SQUARE WAVE PULSES.